Supplementary Information

Film-through large perovskite grains formation via a combination of sequential thermal and solvent treatment

Fan Zhang,‡[ab] Jun Song,‡[a] Linxing Zhang,[a] Fangfang Niu,[a] Yuying Hao,[b] Pengju Zeng,[a] Hanben Niu*[ab] ,Jinsong Huang[c] and Jiarong Lian‡*[a]

[a]. Institute of Optoelectronics, Key Lab of Optoelectronics Devices and Systems of Ministry of Education/Guangdong Province, Shenzhen University, 518060, Shenzhen, China; and Key Laboratory of Micro-Nano Measuring and Imaging in Biomedical Optics, College of Optoelectronic Engineering, Shenzhen University, Shenzhen 518060, China. *E-mail: ljr@szu.edu.cn, niuhb@szu.edu.cn.
[b]. Key Laboratory of Advanced Transducers and Intelligent Control System (Ministry of Education), Taiyuan University of Technology, Taiyuan 030024, China.
[c]. Department of Mechanical and Materials Engineering, Nebraska Center for Materials and Nanoscience, University of Nebraska-Lincoln, Lincoln, Nebraska 68588-0656, USA. *E-mail: jhuang2@unl.edu
† Electronic Supplementary Information (ESI) available: [details of any supplementary information available should be included here]. See DOI: 10.1039/x0xx00000x
‡ These authors contributed equally to this work.

1 Experimental

Material synthesis and purification

First, CH_3NH_3I crystal was synthesized upon reaction of a concentrated aqueous solution of hydroiodic acid (HI) (15.0 ml, 57 wt% in water, Aldrich) with methylamine (CH_3NH_2) (13.5 ml, 40 wt% in aqueous solution, Aldrich) at 0 °C for 2 h with constant stirring under nitrogen atmosphere. The precipitate was recovered by evaporation at 70 °C for 1 h. MAI was dissolved in ethanol at 80 °C, recrystallized from the supersaturated solution at room temperature, and dried at 60 °C in a vacuum oven for 12 h. PbI_2 was bought from Alfa Aesar (99.999%). Clevios PVP AI 4083 poly (3,4-ethylenedioxythiophene) poly (styrenesulphonate) (PEDOT:PSS) was bought from Heraeus (Germany). [6,6]-phenyl-C_{61}-butyric acid methyl ester ($PC_{61}BM$) and 4,7-Diphenyl-1,10-phenanthroline (Bphen) were purchased from Nichem Fine Technology Co. Ltd. (Taiwan). Dimethyl formamide (DMF), dimethyl sulfoxide (DMSO), chlorobenzene (CB) and sec-butyl alcohol were purchased from Sigma-Aldrich (99.5%).

Solar cell fabrication

After cleaning the indium tin oxide (ITO) substrate, a PEDOT: PSS layer was spun on ITO at 2,500 rpm, and then annealed at 125 °C for 15 min.

A perovskite film was deposited on the surface of the PEDOT: PSS layer. The fabrication parameters for different thickness values are summarized in **Table S1;** the fabrication process of the 600-nm-thick film is presented here as an example. The perovskite precursor solution was prepared by mixing 922 mg PbI_2 (99.999%, Alfa Aesar) and 349.8 mg CH_3NH_3I in 0.9 mL of DMF (Sigma-Aldrich) and 0.1 mL of DMSO (Sigma-Aldrich), with PbI_2: CH_3NH_3I molar ratio of 1: 1.1. The mixture solution (70 °C) was spin coated on the PEDOT: PSS layer at 6,000 rpm and, after 7 s of delay time, the wet film was washed with 200 µL of sec-butyl alcohol (washing step). After uniformly dropping sec-butyl alcohol in the center of the substrate, the perovskite film quickly became dark brown. After the spinning stopped, the films were annealed on a hot plate at 100 °C for ~30 s (N_2 atmosphere), quickly becoming black and displaying a mirror-like appearance. The films were then soaked with 200 µL of sec-butyl alcohol for 12 s, and subsequently dried by spin coating at 6,000 rpm for 30 s. The spin-coating process was typically conducted in a glove box under nitrogen atmosphere and with a real-time humidity of ~1 ppm. Finally, the film was subjected to post-annealing treatment (post-annealing step). In this step, the perovskite films were transferred on a hot plate, first annealed in ambient air (real-time humidity of 55%~65%) at 100 °C for 15 min, and then annealed in DMF atmosphere at 100 °C for 15 min. For the DMF atmosphere, a sufficient amount of DMF solvent was dropped into a small ceramic crucible, and then a glass Petri dish was used to cover the samples and crucible.

Subsequently, PCBM was dissolved in chlorobenzene at a concentration of 20 mg/mL and spun on the perovskite layer at 2,500 rpm. Then, the Bphen interfacial layer with concentration of 0.7 mg/mL in ethanol was spin-coated without additional annealing. The devices were completed by evaporating a 100-nm-thick aluminum film as the electrode (active area of 0.12 cm^2).

Characterization

Ultraviolet-visible (UV-vis) light absorption spectra were analyzed to assess the absorption properties of the perovskite film with a UV-vis spectrophotometer (UV-2600). Scanning electron microscopy (SEM) images and X-ray diffraction (XRD) patterns of the films were obtained with a Zeiss Supra 55 microscope and a Bruker QUANTAX 200 diffractometer, respectively. A sun simulator (Zolix Sirius-SS) was used to provide simulated solar irradiation (AM 1.5, 100 mW/cm^2). Current-voltage characteristics were measured using a Keithley 2400 source meter. The output of the light source was adjusted using a calibrated silicon photodiode (ABET technology). The J–V curves were measured by backward—forward bias (1.2 V) → negative bias (−0.5 V)—or forward—negative bias (−0.5 V) → forward bias (1.2 V)—scan. The internal PCE (IPCE) was measured using a power source (Zolix Sirius-SS) with a monochromator (Zolix Omni-λ) and a source meter (Keithley 2400). The device area (12 mm^2) was determined by the overlap of cathode and anode. Notably, the presence of DMSO in the perovskite precursor solution probably alters the charge transport properties of the PEDOT: PSS layer. To avoid overestimation of the photocurrent, an aperture size of 9 mm^2 was used to define the light absorption area.

All devices were measured immediately after fabrication without encapsulation in a super-clean lab with a controlled humidity of 55%~65%.

Table S1. Perovskite film fabrication parameters

Film thickness (nm)	PbI_2, MAI concentration (mole ratio)	DMF:DMSO (v/v)	delay time	sec-butyl alcohol washing step	Soaking time	ambient air annealing time	DMF atmospheres annealing time
~270	1M, 2M (1: 2)	9: 1	7 s	300 μL	12 s	15 min	15 min
~420	1.5M, 2.25M (1: 1.5)	9: 1	7-8 s	300 μL	7 s	15 min	15 min
~650	2M, 2.2M (1: 1.1)	9: 1	8-9 s	200-300 μL	10 s	15 min	15 min
~850	2.25M, 2.43M (1: 1.08)	8.5: 1.5	10 s	400-500 μL	10 s	10 min	25 min
~1020	2.5M, 2.625M (1: 1.05)	8.25: 1.75	10-12 s	500-600 μL	10 s	5 min	35 min

2 Grain-size distributions of the perovskite films obtained at different pre-annealing temperatures

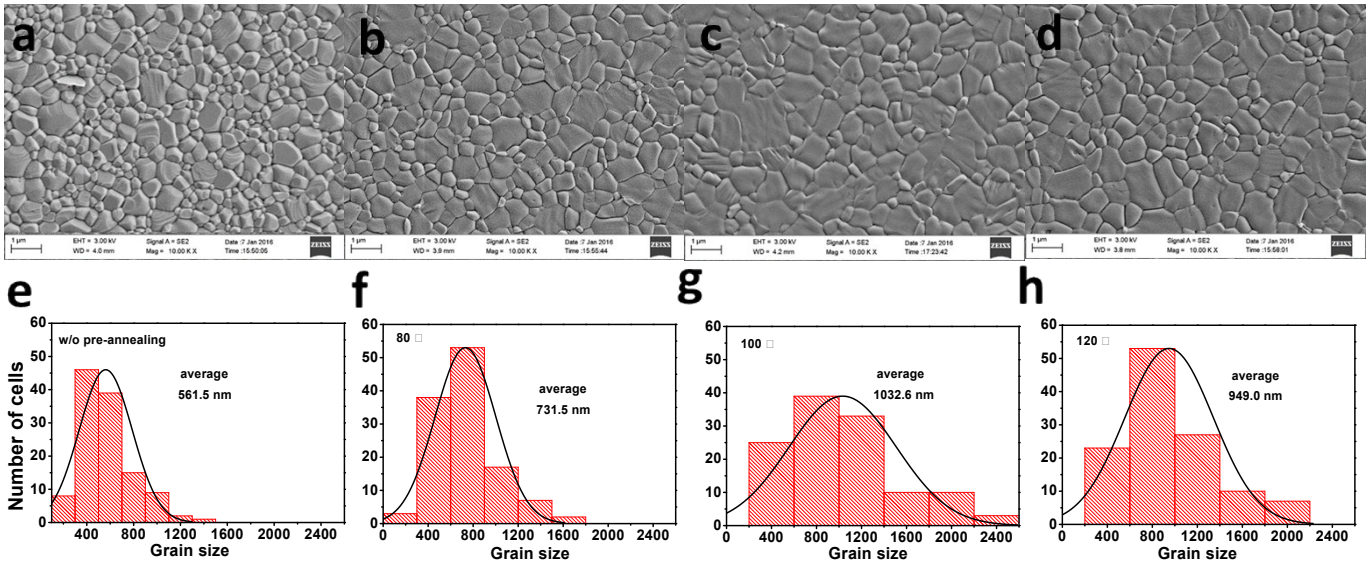

Figure S1. Surface SEM image of perovskite films obtained at different pre-annealing temperatures and grain-size distributions of the same films: (a, e) without pre-annealing step, (b, f) 80 °C, (c, g) 100 °C, (d, h) 120 °C.

3 Photovoltaic performance of perovskite solar cells with different pre-annealing temperatures

Table 1 Photovoltaic performance of perovskite solar cells with different pre-annealing temperature. Average values were obtained from 6 cells.

Pre-annealing temperature (°C)	J_{SC} (mA/cm2)	V_{OC} (V)	FF	PCE (%)
w/o	20.48 ± 1.50	0.871 ± 0.035	0.704 ± 0.021	12.41 ± 1.08
80	21.91 ± 0.39	0.958 ± 0.008	0.756 ± 0.012	15.69 ± 0.67
100	22.25 ± 0.32	0.972 ± 0.008	0.766 ± 0.007	16.58 ± 0.46
120	20.19 ± 0.47	0.974 ± 0.004	0.748 ± 0.022	14.87 ± 0.50

4 J-V curves of devices with different pre-annealing temperatures

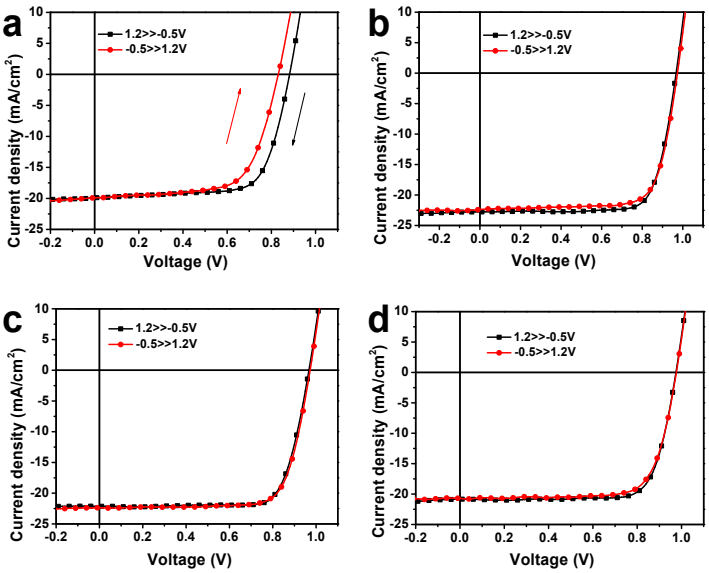

Figure. S2 J-V curves of devices with different pre-annealing temperatures: (e) without pre-annealing step, (f) 80 °C, (g) 100 °C, and (h) 120 °C, measured using forward and backward scans.

In the literature, it has been often reported that the current density–voltage (J-V) curves of perovskite solar cells obtained from forward scan (FS, the scan from lower to higher voltage) and reverse scan (RS, the scan from higher to lower voltage) were not consistent. This phenomenon is called hysteresis, and often occurs in perovskite devices, depending on their quality and architecture. Figure S2(a–d) shows the J–V curves of the devices, which are close to the average results obtained under each condition, measured under forward and reverse scans.

5 J-V curves of devices with different scan rates

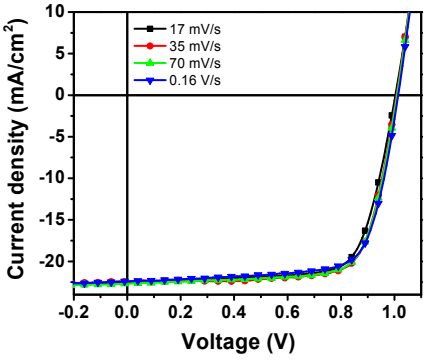

Figure. S3 J-V curves of device with different scanning rates measured from negative to positive bias.

6 PL spectra of perovskite films with different pre-annealing temperatures

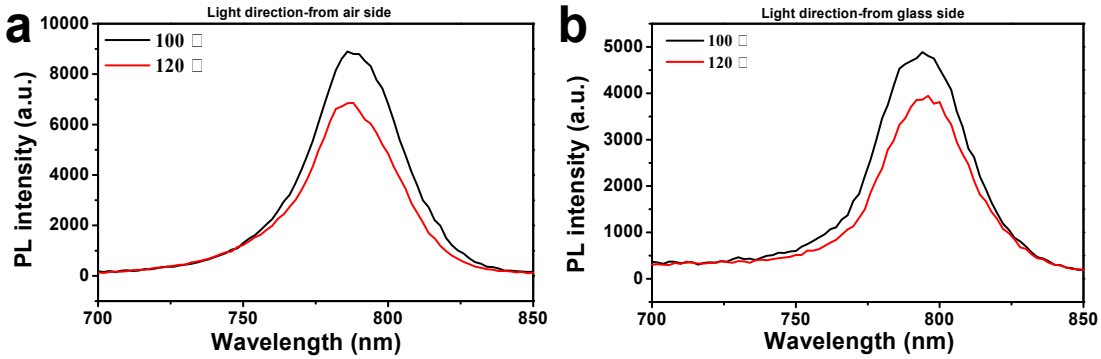

Figure. S4 PL spectra of $CH_3NH_3PbI_3$ film prepared with different pre-annealing temperatures. An excitation light of 325 nm falls on the perovskite films from the air side (a) and glass side (b), respectively.

7 J-V curves and EQE spectra of perovskite solar cell devices with perovskite films of different thicknesses

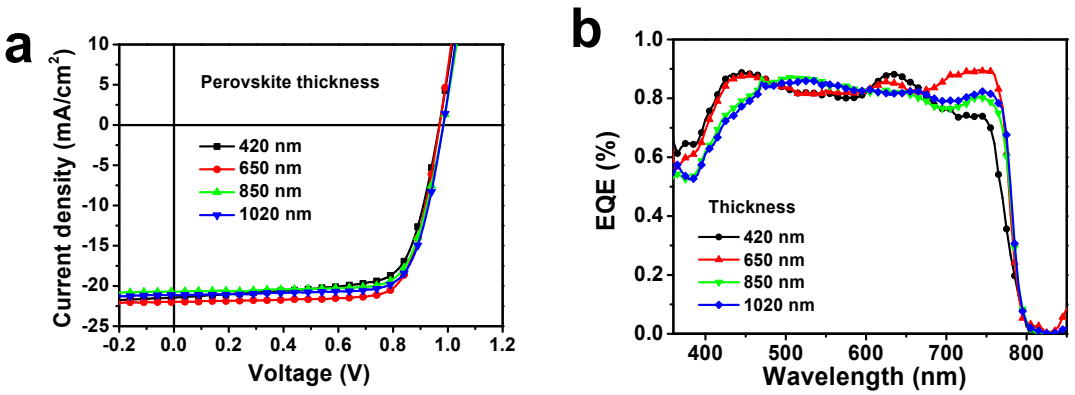

Figure. S5 J-V curves (a) and EQE spectra (b) of perovskite solar cell devices with perovskite films of different thicknesses.